A PHOTOMETRIC STUDY OF THE GLOBULAR CLUSTER M54 AND THE SAGITTARIUS DWARF GALAXY: EVIDENCE FOR THREE DISTINCT POPULATIONS

ATA SARAJEDINI
Kitt Peak National Observatory, National Optical Astronomy Observatories,[1] P.O. Box 26732, Tucson, Arizona 85726
Electronic mail: ata@noao.edu

ANDREW C. LAYDEN
Cerro Tololo Inter-American Observatory, National Optical Astronomy Observatories, Casilla 603, La Serena, Chile
Electronic mail: alayden@noao.edu

Received 1994 October 18; revised 1994 November 23

ABSTRACT

We present *VI* CCD color–magnitude diagrams for the globular cluster M54 and the Sagittarius dwarf galaxy. These are used to derive the following quantities: [Fe/H]$=-1.79\pm0.08$ for M54 and [Fe/H]$=-0.52\pm0.09$ for Sagittarius. We find a metallicity dispersion of ±0.16 dex in M54, and we infer the possible existence of a [Fe/H]≈-1.3 component in Sagittarius, which may have a metallicity dispersion as well. The mean reddening in the direction of M54 is $E(B-V)=0.13\pm0.02$. The distances to M54 and Sagittarius, determined using their horizontal branch magnitudes, are identical to within the uncertainties of existing RR Lyrae luminosity–abundance relations. This, together with positional and radial velocity arguments, suggests that M54 is physically associated with Sagittarius. We note that M54 is substantially brighter than the globular cluster members of the Fornax dwarf spheroidal galaxy, and that the metal abundance of Sagittarius is quite high for its estimated absolute magnitude.

1. INTRODUCTION

Ibata *et al.* (1994, hereafter referred to as IGI) have reported the discovery of a Local Group dwarf galaxy located in the constellation of Sagittarius. It is the closest such object yet identified and it is located on the opposite side of the galactic center. Thus, Sagittarius (Sgr) joins the growing list of Milky Way satellite galaxies, becoming the 11th such object known. However, IGI find the distribution of stars in Sgr to be extremely clumpy, unlike other dwarf spheroidal (dSph) galaxies. They took this, together with its proximity to our galaxy, to indicate that Sgr is in the process of being tidally disrupted and accreted by the Galaxy.

Mateo *et al.* (1995, hereafter referred to as MUSKKK) present a *VI* color–magnitude diagram for Sgr and a control field devoid of Sgr stars. After statistically subtracting the control field stars, they find the dominant Sgr population to be roughly 10 Gyr old. They estimate [Fe/H]$\approx-1.1\pm0.3$ dex, from the color of the red giant branch. They also find a handful of RR Lyrae variables, suggesting that Sgr also possesses an older and/or more metal-poor population.

IGI noted that the globular cluster NGC 6715 (M54) lies in the densest clump of the Sgr dwarf galaxy. The only previous color–magnitude diagram (CMD) of this cluster was constructed by Harris (1975), and was based on photographic plates. The CMD reached the cluster horizontal branch (HB) at $V\approx17.7$, and indicated a foreground reddening of $E(B-V)=0.17$. Throughout the magnitude range of interest, the photometric errors and the degree of field contamination were sufficient to mask any features that could be attributed to another stellar system, such as the red giant branch (RGB) of a dwarf galaxy.

Given the exciting discovery of the Sgr dSph, it is clear that CCD-based photometry is urgently needed for the field around M54. We present a *VI* CCD photometric study of the globular cluster M54 and the Sgr dwarf galaxy, using, as our analytical tools, the *VI* photometry of globular cluster RGBs from DaCosta & Armandroff (1990, hereafter referred to as DCA) and the simultaneous reddening and metallicity (SRM) method devised by Sarajedini (1994). In the next section, we describe the observational setup and reduction procedure. The CMDs derived from the photometric data are presented in Sec. 4. The results of the SRM method are described and discussed in Secs. 5 and 6, respectively.

2. OBSERVATIONS

Observations of M54 were made on 1994 June 16/17 and 17/18, using the CTIO 0.9 m telescope and the Tektronix #2 CCD, readout in a four-amplifier mode by the ArCon controller. The CCD is a 1024×1024 array (Tek1024) having 24 μm pixels, corresponding to 0.4 arcsec pixel^{-1}. The readout noise was five electrons. The CTIO "Tek 2" *V* filter, and the "KC#32" *I* filter were used. Conditions were photometric on both nights. Three *VI* frame pairs were obtained of the cluster on each night, and four *VI* pairs of a field centered 12 arcmin north of the cluster were obtained on the second night. The seeing varied from 1.4 to 1.9 arcsec FWHM. Figure 1 (Plate 30) shows a *V* band reproduction of the observed M54 field and Fig. 2 (Plate 31) shows the off-cluster field. Standard stars from Landolt (1992) were observed throughout both nights, covering a range of colors and airmasses.

---

[1]NOAO is operated by the Association of Universities for Research in Astronomy, Inc., under contract with the National Science Foundation.

The frames were overscan corrected and trimmed using the CTIO IRAF[2] package QUADPROC. Twilight sky flats were used to flat field the data. These were effective in removing the quadrant-to-quadrant gain variations produced by the four separate amplifiers to better than 0.5%.

Seven more *VI* frame pairs were obtained of the cluster on 1994 June 25/26 and 26/27, using the 0.9 m telescope and the newly commissioned Tektronix ♯4 2048×2048 chip (Tek2048), also read in the four-amplifier mode by ArCon. This chip has a field of view of 13.5 arcmin at a scale of 0.4 arcsec pixel^{-1}, and was operated with a read noise of four electrons. These nights were not photometric, and the seeing varied from 1.3 to 2.0 arcsec FWHM. Unfortunately, after flat fielding with twilight sky flats, it was found that many of the object frames showed low-order sky background variations at the 2%–3% level. The degree of nonflatness increased with time during a night. This effect was later attributed to outgassing of new components in the dewar; material condensed on the cold CCD to create a thin, color-dependent film that grew thicker with time.

Since these large-format frames would greatly increase the number of stars in our program, particularly stars in the background dwarf galaxy, we decided to attempt a correction of this low-level nonflatness. Many of our frames, observed for a different project, had low stellar densities and sufficient sky backgrounds that we could combine them to produce correction sky flats. We grouped together *V* and *I* frames into blocks of approximately 2 h, and combined them using the IRAF task FLATCOMBINE in the CCDRED package. We then BOXCAR smoothed the resulting image by 40–50 pixels to improve the signal-to-noise, and divided by the mean counts in the frame. Then, we divided the individual cluster images by the correction image nearest in time of observation. The corrected cluster *V* images appeared flat to about 1% or better across the chip. The correction of the *I* images was less successful (typically flat to 1%–2%) since fewer *I* images were available as a function of time to make the correction images.

3. REDUCTIONS

3.1. Standard Stars

The standard star solutions were computed separately for the two photometric nights, giving two independent calibrations. These are of the form

$$i-I=a_I+b_I(V-I)+c_IX_I+d_IX_I(V-I)+e_I\mathrm{HJD}_I \quad (1)$$

$$(v-i)-(V-I)=a_{V-I}+c_{V-I}X_{V-I}. \quad (2)$$

In this formulation, v and i refer to the instrumental magnitudes (corrected for exposure time), V, I, and $(V-I)$ are the standard system values, X is the airmass of each observation, and HJD is the fractional part of the heliocentric Julian date. For the 20 to 30 standard stars observed on each of the two photometric nights, the root-mean-square (RMS) deviations of the standard values from the fits were 0.006 and 0.011 mag for $i-I$, and 0.012 and 0.015 mag for $(v-i)-(V-I)$.

3.2. Program Objects

The reader is referred to Sarajedini & Milone (1995, and references therein) for a full description of the reduction procedure applied to the program images using DAOPHOT II (Stetson 1987). We note only that, in the present case, between 120 and 200 uncrowded stars were used to construct the point-spread function (PSF) for each frame. The final instrumental magnitudes were edited using the image diagnostics output by DAOPHOT and matched to form colors. In the case of data obtained under photometric conditions, aperture corrections, determined using DAOGROW (Stetson 1990), were applied to the PSF magnitudes, and the resultant photometry was transformed to the standard system using Eqs. (1) and (2) (see Sarajedini & Da Costa 1991). Magnitude offsets between each frame pair and the mean photometric zeropoint were never greater than ±0.02 mag. In particular, for the six Tek1024 frames centered on M54, the standard deviation of these offsets, derived by applying the small sample statistical formulae of Keeping (1962), was 0.015 mag, which we adopt as the uncertainty in our photometric zeropoint. The final step in the reduction of the photometric data involved adjusting the zero point of each frame pair to the mean photometric zero point and averaging the colors and magnitudes of stars in common between the frames, weighted by the inverse square of their errors. The error in each V and $V-I$ measurement is based on the frame-to-frame scatter in these values. More specifically, we adopt the standard error of the mean, determined using the formulae of Keeping (1962), as the 1σ uncertainty of each measurement.

The reduction of the nonphotometric observations (June 25/26 and 26/27) was identical to those obtained under photometric conditions, except for the transformation to the standard system. For each nonphotometric frame pair, we used the photometric data to solve for the coefficients in the following equations:

$$V-I=a_{V-I}+b_{V-I}(v-i)+c_{V-I}X+d_{V-I}X^2+e_{V-I}Y+f_{V-I}Y^2, \quad (3)$$

$$v=V+a_V+b_V(V-I)+c_VX+d_VX^2+e_VY+f_VY^2, \quad (4)$$

where X and Y represent the pixel position of each star on the frame. This spatial component to the photometric fit was necessitated by the difficulty experienced in flat fielding the CCD frames. It is because of this problem that we have decided not to combine the photometric and nonphotometric observations into one master set of data, preferring instead to keep them separate in order to maintain the integrity of our photometric scale.

4. COLOR–MAGNITUDE DIAGRAMS

Figure 3 shows the CMD of 3214 stars derived from the Tek1024 CCD frames of the field around M54 (see Fig. 1). These data are listed in Table 1. Figure 4 shows the CMD of

[2]IRAF is distributed by the National Optical Astronomy Observatories, which are operated by the Association of Universities for Research in Astronomy, Inc. under cooperative agreement with the National Science Foundation.

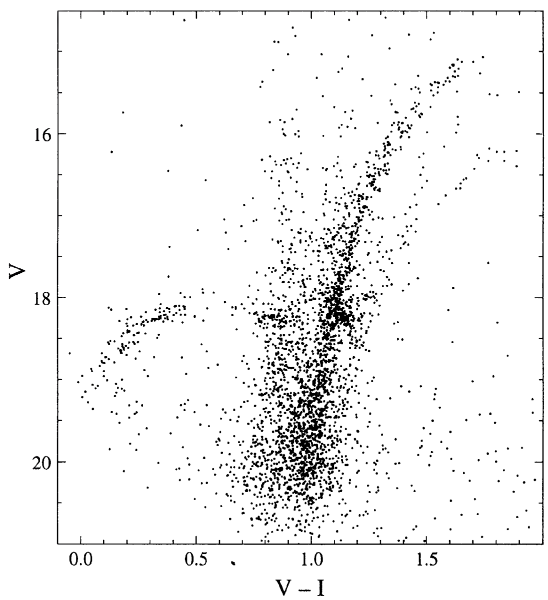

FIG. 3. Color–magnitude diagram of 3124 stars in the direction of M54 obtained with the Tek1024 CCD. Only stars with at least three detections, $\sigma_V \leqslant 0.050$ mag and $\sigma_{V-I} \leqslant 0.071$ mag have been plotted.

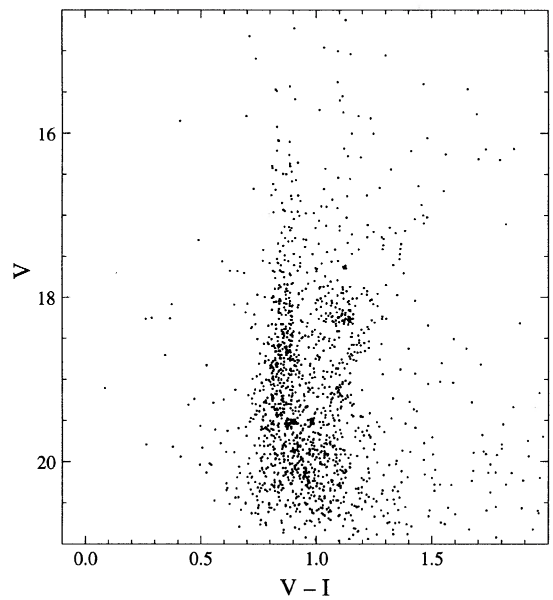

FIG. 4. Color–magnitude diagram of 1638 stars in a region located 12 arcmin north of M54 obtained with the Tek1024 CCD. Only stars with at least three detections, $\sigma_V \leqslant 0.05$ mag and $\sigma_{V-I} \leqslant 0.071$ mag have been plotted.

1638 stars in the field 12 arcmin north of M54 (see Fig. 2). These data are listed in Table 2. In both CMDs, only stars with at least three detections, $\sigma_V \leqslant 0.050$ mag, and $\sigma_{V-I} \leqslant 0.071$ mag are plotted. In Fig. 3, we see a well-populated, fairly steep RGB with $V_{\rm tip} \approx 15.2$ and $(V-I)_{\rm tip} \approx 1.7$, along with a well-defined blue HB (BHB). These must belong to M54, since they do not appear in the off-cluster CMD in Fig. 4. Figure 3 also shows another RGB sequence with $V_{\rm tip} \approx 16.2$ and $(V-I)_{\rm tip} \approx 1.9$, in addition to a red HB clump, which partially overlaps the RGB of M54. These features are similar to those shown in Fig. 2 of IGI and MUSKKK, and we therefore associate them with Sgr. Our Fig. 4 also exhibits these sequences, but they are less densely populated. The ratio of the Sgr RGB star densities in Figs. 3 and 4 are consistent with the density ratio predicted from the IGI isopleth map. Returning to the morphology of Fig. 3, there is a red HB (RHB) at $V \approx 18.3$ and $V-I \approx 0.85$, which appears weak or absent in Fig. 4; we will discuss whether it

TABLE 1. CCD photometry for M54 and Sgr.[a]

#	X	Y	V	σ_V	$V-I$	σ_{V-I}	N
1	501.29	355.34	12.64	0.005	1.13	0.010	6
2	169.72	688.89	13.10	0.005	1.13	0.006	6
3	391.69	257.26	13.55	0.003	1.33	0.006	6
4	1063.44	628.40	13.56	0.004	0.92	0.009	3
5	511.92	165.07	13.78	0.004	0.76	0.002	6
6	404.06	564.12	13.81	0.004	0.64	0.009	6
7	550.53	374.17	13.82	0.004	1.26	0.005	6
8	257.04	621.25	13.82	0.004	0.80	0.001	6
9	571.59	176.43	14.10	0.007	1.21	0.006	6
10	753.23	209.24	14.19	0.005	1.09	0.006	6
11	310.48	886.18	14.19	0.004	1.10	0.003	6
12	36.67	164.91	14.23	0.003	1.20	0.005	3
13	106.00	575.09	14.29	0.007	1.03	0.005	6
14	110.72	328.20	14.34	0.002	1.14	0.009	6
15	72.40	480.80	14.58	0.004	1.32	0.004	5
16	1028.70	760.39	14.61	0.003	1.16	0.002	3
17	1054.65	831.93	14.61	0.008	0.45	0.006	3
18	410.13	276.87	14.70	0.003	0.92	0.003	6
19	160.76	503.84	14.77	0.004	1.53	0.003	6
20	508.53	1067.16	14.79	0.008	1.42	0.004	4
21	66.79	988.81	14.80	0.007	1.26	0.006	5
22	398.81	255.49	14.81	0.005	0.93	0.003	5
23	470.38	398.63	14.85	0.044	1.52	0.024	3
24	758.71	978.42	14.88	0.014	0.84	0.009	6
25	169.62	112.09	14.88	0.002	0.86	0.003	6
26	376.87	765.13	14.96	0.003	1.34	0.003	6
27	543.33	385.48	15.03	0.008	1.04	0.007	6
28	465.75	790.99	15.03	0.005	0.90	0.002	6
29	315.03	844.84	15.06	0.003	1.16	0.002	6
30	334.28	331.99	15.06	0.005	1.74	0.002	6

[a]Table 1 is to be presented in its complete form in the ApJ/AJ CD-ROM Series. The first page of this table is presented here for guidance regarding its form and content.

TABLE 2. CCD photometry for Sgr.[a]

#	X	Y	V	σ_V	$V-I$	σ_{V-I}	N
1	494.75	871.28	12.91	0.000	1.21	0.003	4
2	635.26	322.61	13.99	0.000	1.38	0.003	4
3	781.15	899.89	14.07	0.001	1.33	0.002	4
4	344.20	260.02	14.10	0.003	1.03	0.006	4
5	999.11	749.08	14.24	0.002	0.98	0.005	4
6	69.00	1009.58	14.31	0.001	1.47	0.003	4
7	392.49	917.76	14.41	0.001	0.91	0.003	4
8	862.69	599.88	14.42	0.001	1.33	0.001	4
9	705.37	711.17	14.62	0.001	1.13	0.002	4
10	743.66	382.86	14.72	0.000	0.90	0.006	3
11	424.06	443.70	14.82	0.002	0.71	0.006	4
12	794.54	599.88	14.85	0.001	3.08	0.002	3
13	349.18	800.05	14.96	0.000	1.03	0.001	4
14	653.28	538.73	15.00	0.001	1.09	0.002	4
15	348.29	437.10	15.03	0.002	1.15	0.004	4
16	1022.00	693.87	15.05	0.004	1.30	0.002	4
17	584.24	212.65	15.09	0.002	0.74	0.004	4
18	260.14	256.24	15.37	0.002	1.09	0.002	3
19	87.76	674.98	15.40	0.002	1.46	0.005	3
20	833.84	152.64	15.42	0.000	0.88	0.004	4
21	113.22	48.82	15.46	0.002	1.65	0.004	4
22	762.01	783.22	15.47	0.000	0.82	0.002	4
23	14.65	404.00	15.48	0.002	0.83	0.006	4
24	735.42	844.69	15.55	0.002	1.11	0.001	4
25	278.76	875.32	15.58	0.001	0.91	0.004	3
26	469.52	159.02	15.60	0.002	1.10	0.005	4
27	104.52	542.67	15.71	0.001	1.01	0.002	4
28	208.22	207.19	15.74	0.000	1.12	0.003	3
29	218.05	877.94	15.76	0.000	1.69	0.002	4
30	806.45	816.06	15.79	0.002	1.18	0.002	4

[a]Table 2 is to be presented in its complete form in the ApJ/AJ CD-ROM Series. The first page of this table is presented here for guidance regarding its form and content.

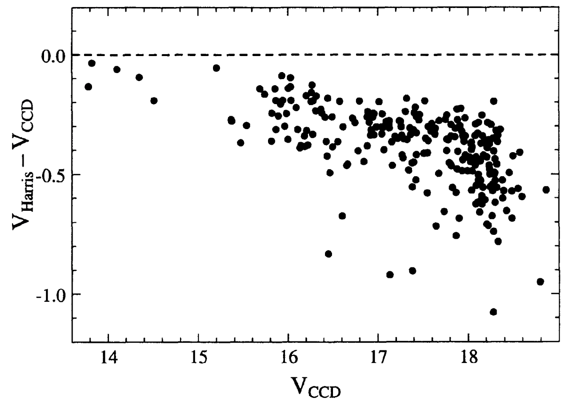

FIG. 5. Star-by-star comparison of the CCD photometry shown in Fig. 3 with the photographic photometry of Harris (1975).

belongs to M54 or Sgr in Sec. 6. The signature of field star contamination is also evident in both Figs. 3 and 4. This is due to the foreground disk and bulge, primarily forming a vertical sequence at $0.7 \lesssim V-I \lesssim 1.3$, with redder stars at both the brightest and faintest regions of the CMDs. This feature is also present in the CMDs of IGI and MUSKKK.

We have photometry for 16 of the 21 *confirmed* RR Lyrae variables in M54, as listed by Sawyer-Hogg (1973). The mean magnitude of these stars from our photometry is $\langle V(\mathrm{RR}) \rangle = 18.17 \pm 0.05$ mag. We can estimate the fraction of these stars that belong to Sgr as follows. MUSKKK found 6–7 Sgr RR Lyraes in a 15 arcmin-square field at $(l,b) = (6.63, -16.27)$. Normalizing by the ratio of the HB star densities in the two fields, as estimated from the IGI isopleth map, and accounting for our smaller CCD field, we expect 1–3 of the 16 stars to belong to Sgr. This small degree of contamination should not significantly affect the determination of the mean magnitude of the M54 variables. We therefore adopt $\langle V(\mathrm{RR}) \rangle = 18.17 \pm 0.05$ as the HB magnitude of M54. Note that this is significantly different from Harris' (1975) photographic value of 17.71 mag. The reason for this is illustrated via a star-by-star comparison of our photometry with that of Harris (1975). Figure 5 shows the difference between the two V magnitudes ($V_{\mathrm{Harris}} - V_{\mathrm{CCD}}$) as a function of V from the present work (V_{CCD}). It is clear that there is an offset of ≈ 0.1 mag, even for the brightest stars. At $V_{\mathrm{CCD}} \approx 18$, the mean offset is ≈ -0.4, which explains the difference between the derived RR Lyrae magnitudes. We note that several of Harris' photoelectric standards fall on our Tek2048 frames; the colors and magnitudes are in agreement to within the accuracy of our Tek2048 photometry.

For the anonymous RHB, the stars in Fig. 3 with $0.75 \leqslant V - I \leqslant 1.0$ and $18.1 \leqslant V \leqslant 18.4$ yield a mean magnitude of $V(\mathrm{RHB}) = 18.25 \pm 0.05$. For the Sgr red clump, we consider all the stars in Fig. 4 with $1.05 \leqslant V-I \leqslant 1.17$ and $18.1 \leqslant V \leqslant 18.4$; we find a mean value of $V(\mathrm{clump}) = 18.24 \pm 0.02$. The uncertainties in $V(\mathrm{RHB})$, $V(\mathrm{clump})$, and $\langle V(\mathrm{RR}) \rangle$ are each composed of the corresponding standard error of the mean, together with the error in the photometric zeropoint of ± 0.015 mag (*Sec. 3.2*). The temporal coverage of our off-cluster frames was insufficient to detect RR Lyrae candidates in Sgr.

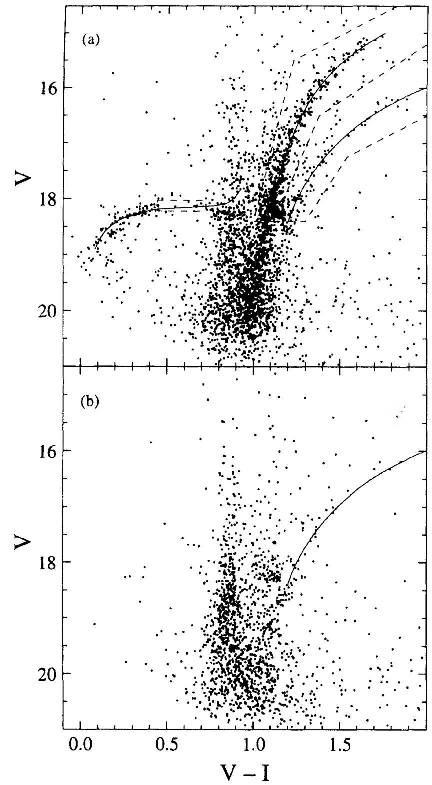

FIG. 6. (a) The same as Fig. 3, except that the solid lines are the adopted red giant branches of M54 (left) and the Sagittarius dwarf galaxy (right). The dashed lines represent the regions over which the polynomials that define the giant branches have been fitted. The HB fiducial of M68 (Walker 1994) has been fitted to the BHB stars. The dashed box superimposed on the fiducial marks the locus of Walker's RR Lyrae stars. (b) The same as Fig. 4, except that the solid line represents the red giant branch of Sgr derived from the data in Fig. 3 and also plotted in (a).

The color of the RGB at the level of the HB is measured in the following manner, which is also described in Sarajedini & Norris (1994, hereafter referred to as SN94). We have used an iterative 2σ rejection fitting scheme to fit polynomials to the stars in the two dotted regions of Fig. 6(a); the left/upper region corresponds to M54 and the right/lower region to Sgr. The solid lines show the resultant fits, both of which are quite reasonable. The RGB fit for Sgr has also been plotted in Fig. 6(b), where, as one would expect, it is a satisfactory match to these data. Thus, at the HB levels quoted above, we determine $(V-I)_{g,\mathrm{M54}} = 1.095 \pm 0.015$ and $(V-I)_{g,\mathrm{Sgr}} = 1.218 \pm 0.016$. The error in each value of $(V-I)_g$ has been computed by considering only stars used in the RGB fit with V magnitudes in the range used to compute $V(\mathrm{HB})$. The standard error in $V-I$ of these stars from the fit combined with the uncertainty in the photometric zeropoint of ± 0.015 mag constitutes the adopted error in $(V-I)_g$ (see SN94).

The problems encountered with flattening the Tek2048 images have been described above. Even though these data are not as well calibrated as those obtained with the Tek1024

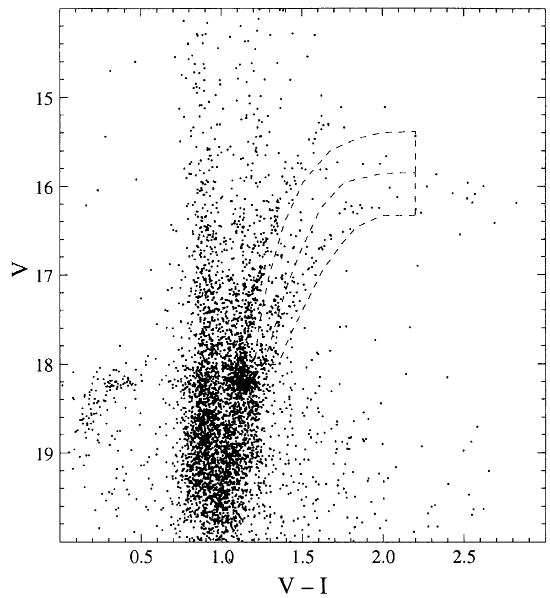

FIG. 7. Color–magnitude diagram of 4790 stars in the direction of M54 obtained with the Tek2048 CCD. Only stars with at least three detections, $\sigma_V \leq 0.05$ mag, $\sigma_{V-I} \leq 0.071$ mag, and located more than 2′ from the center of M54 are shown. The dashed regions are described in the text.

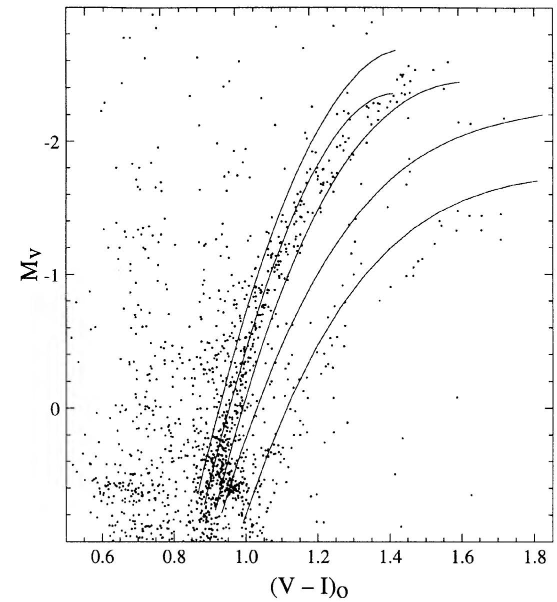

FIG. 8. Standard red giant branches from Da Costa & Armandroff (1990), along with the data in Fig. 3 dereddened by 0.18 and shifted to the same distance, assuming the derived V(HB), [Fe/H], and M_V(HB)=0.17[Fe/H]+0.82. From left to right, the standard sequences are those of M15, NGC 6397, M2, NGC 1851, and 47 Tuc, with metallicities of −2.17, −1.91, −1.58, −1.29, and −0.71, respectively.

detector, they do cover a larger area in the sky. Figure 7 shows the CMD for 4790 stars with at least 3 detections, $\sigma_V \leq 0.050$ mag, $\sigma_{V-I} \leq 0.071$ mag, and located more than 2′ from the center of M54. First, note the large number of very red stars that form an extension of the Sgr RGB, including four unplotted stars with $3.0 \leq V-I \leq 4.0$. As we shall see below, these are indicative of the metal-rich nature of Sgr, reminiscent of the CMDs of metal-rich Galactic globular clusters published by Bica *et al.* (1994, and references therein).

5. REDDENINGS AND METALLICITIES

5.1. *The SRM Method*

Since we have constructed RGBs for both M54 and the Sgr dwarf, and, in addition, computed their V(HB) and $(V-I)_g$ values, it is now possible to apply the simultaneous reddening and metallicity (SRM) technique of Sarajedini (1994, hereafter S94). Using the "numerical solution" described by S94, we derive [Fe/H]=−1.79±0.08 and E($B-V$)=0.13±0.02 for M54 and [Fe/H]=−0.52±0.09 and E($B-V$)=0.13±0.02 for the Sgr dwarf galaxy. The conversion to E($B-V$) from E($V-I$) has been accomplished using the relation of Dean *et al.* (1978). Note that the metallicity of Sgr is formally greater than the most metal-rich calibrator used by S94, necessitating a slight extrapolation. However, given the predominantly linear behavior of $(B-V)_{0,g}$ with [Fe/H] over a metallicity range extending from the most metal-poor globular clusters to [Fe/H]≈−0.3 (Zinn & West 1984; SN94), we expect $(V-I)_{0,g}$ to behave similarly. Figure 8 shows the standard $[M_V,(V-I)_0]$ giant branches of DCA along with the photometry in Fig. 3, which has been dereddened by E($V-I$)=0.18 and shifted to the same distance scale using V(HB)=18.17, [Fe/H]=−1.79, and M_V(HB)=0.17[Fe/H]+0.82. It is clear from Fig. 8 that the quantities derived via the SRM method are consistent with the RGB fiducials of these clusters. Furthermore, DCA predict the brightest cluster giant star at [Fe/H]=−1.79 to have $M_{\rm bol}=-3.47$, while we find $M_{\rm bol}=-3.54$ for M54. Given the scatter among the values of $M_{\rm bol}$ computed by DCA, the M54 values are in reasonable accord.

5.2. *A Metallicity Spread in M54?*

The reader will notice that the M54 RGB shown in Fig. 3 appears rather wider than indicated by the photometric errors. This could be due to differential reddening across the face of the cluster or an intrinsic spread in the abundances of the M54 giant stars. To test the first possibility, we modeled the color of each RGB star in terms of its magnitude and (x,y) position on the CCD frames (Cudworth & Rees 1990). The coefficients of the x and y terms were not statistically significant, implying that the effect of differential reddening is unimportant.

To explore the second possibility, we examined the color difference between each M54 giant star in the range $15.0<V<17.5$ and the M54 RGB fiducial plotted in Fig. 6(a). This particular magnitude range was chosen because the photometric errors, as defined by the frame-to-frame scatter of the photometric measurements, are relatively constant. A histogram of these color differences $[\delta_{V-I} \equiv (V-I)_{\rm obs}-(V-I)_{\rm fit}]$ is shown with filled circles in Fig. 9, where the open circles include only stars located inside 2 arcmin of the cluster center. The solid and dashed lines are Gaussian fits to the points with $\delta_{V-I}>-0.03$ mag. This range was chosen so as to mini-

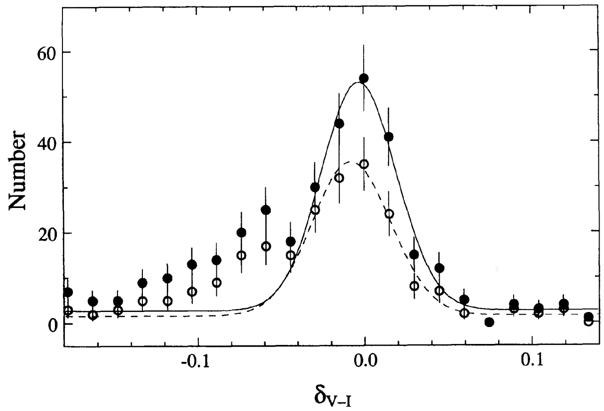

FIG. 9. The filled circles represent the histogram of the distribution of color differences between each giant star in the range $15.0<V<17.5$, and the M54 RGB fiducial shown in Fig. 6(a). The open circles include only stars located inside 2 arcmin of the cluster center.

mize the effects of asymptotic giant branch stars, whose distribution peaks at $\delta_{V-I}\approx-0.06$ mag. The standard deviations, $\sigma_{\rm total}$, of the solid and dashed curves are 0.0225 ±0.0013 mag and 0.0236 ± 0.0015 mag, respectively.

How much of this dispersion is due to photometric error in $V-I$? To answer this question satisfactorily, we must rely on artificial star experiments. For each of the Tek1024 CCD frames centered on M54, a total of 2000 artificial stars were generated with colors and magnitudes lying on the M54 RGB fiducial. These were then added to the original frames, 400 at a time, and reduced in exactly the same manner as the real stars. After all of the editing, matching, and transforming to the standard system was accomplished, 1764 stars remained. Histograms of color differences from the M54 RGB were constructed for all recovered artificial stars, and the 488 stars located inside 2 arcmin of the cluster center. Gaussian fits to these distributions yielded standard deviations, σ_{V-I}, of 0.0044 ± 0.0002 mag for all stars and 0.0070 ± 0.0004 for those inside 2 arcmin. These dispersions represent the contribution of photometric error (photon noise and crowding) to the distributions plotted in Fig. 9. Assuming that $\sigma^2_{\rm total}=\sigma^2_{V-I}+\sigma^2_{\rm [Fe/H]}$, we find that the dispersion in color produced by the intrinsic scatter in abundance, $\sigma_{\rm [Fe/H]}$, is 0.0221 ±0.0013 mag for all stars, and 0.0225 ± 0.0016 for those inside 2 arcmin. What do these correspond to in terms of [Fe/H]? Using the DCA RGBs of M15 ([Fe/H]$=-2.17$), NGC 6397 (-1.91), and M2 (-1.58) at $M_V=-1$, these translate to a metallicity dispersion of $\pm0.16\pm0.01$ dex in M54. This result should be confirmed by high-quality spectroscopic abundance measurements.

5.3. Comparisons with Previous Results

Our mean abundance of [Fe/H]$=-1.79$ for M54 is substantially lower than that of Zinn & West (1984), who derived [Fe/H]$=-1.42\pm0.15$. Their abundance is based on the Q_{39} integrated-light index. Our derived reddening is somewhat less than that quoted by Harris, who found $E(B-V)=0.17$ from the mean color of the RR Lyraes in his data. However, we have already questioned Harris' photographic HB magnitude determination, so a color error of a few hundredths of a magnitude is quite plausible. The Burstein & Heiles (1982) reddening maps predict $E(B-V)=0.14$, while MUSKKK found $E(B-V)=0.18\pm0.03$ in a field $\approx1°$ from ours.

MUSKKK derived a metal abundance of [Fe/H]$=-1.1$ ±0.3 for Sgr. Formally, this is only 1.9σ different from our value. However, a glance at their Fig. 2 reveals that their Sgr RGB actually crosses two of DCAs standard RGBs.[3] This suggests that if a smaller reddening was adopted, their Sgr RGB would lie redward of its present location and imply a metallicity closer to ours. In fact, if we apply the SRM method to MUSKKKs photometry, we find [Fe/H]$=-0.74$ ±0.06 and $E(B-V)=0.10\pm0.03$. We note that these errors are probably underestimates of the true errors because of the difficulty in isolating the actual RGB of Sgr in Fig. 1 of MUSKKK. The discrepancy between the reddening derived via the SRM method [$E(B-V)=0.10\pm0.03$] and that quoted by MUSKKK [$E(B-V)=0.18\pm0.03$] is not formally significant (1.9σ). However, the difference is either due to an actual difference in the foreground reddening or in the photometric zeropoints.

6. DISCUSSION

Does the anonymous RHB in Fig. 3 belong to M54 or to Sgr? This has important implications for the relative distances of these populations, as well as for the stellar population content of Sgr. One method we can use to answer this question involves applying a statistical field subtraction, like that employed by MUSKKK, to our Figs. 3 and 4. However, a more quantitative measure can be obtained by deriving luminosity functions (LFs) in a narrow color range encompassing the RHB, $0.75\leq V-I\leq1.00$ in our Fig. 7 data, and $0.70\leq V-I\leq0.95$ in the MUSKKK data. These color ranges are slightly different, due to possible differences in the photometric zeropoints and/or the reddenings. Figure 10 shows these LFs for the MUSKKK Sgr field (open circles) and their control field (filled circles; see Fig. 1 of MUSKKK). The open squares are the LF of the data in our Fig. 7, while the triangles represent the off-cluster field whose CMD is shown in Fig. 4. These LFs have been scaled vertically over $15<V<18$ mag in order to normalize the star counts from the different-sized CCD fields and the different stellar density environments. In the range $18.1<V<18.3$, there is clearly an enhancement in the LFs that include Sgr, whereas the control field shows no such enhancement. This indicates that the RHB present in Figs. 3 and 7 is also evident in the CMD of Sgr from MUSKKK, but does not exist in the foreground field population. This is one piece of evidence suggesting that the RHB belongs to Sgr, and not M54. With regard to the LF of Fig. 4, we note that an enhancement is seen at $V\approx18.2$, but because the data comes from a region of the sky

[3]Mateo (private communication) notes that the brightest stars near the tip of the Sgr RGB in MUSKKKs photometry may be incomplete, and their photometry may be of questionable accuracy because they were near the saturation limit of their detector.

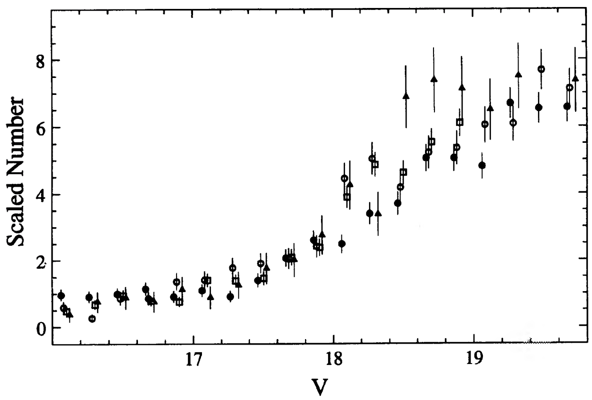

FIG. 10. The luminosity function for the stars shown in Fig. 7 with $0.75 \leq V - I \leq 1.00$ (open squares), for our Sgr field shown in Fig. 4 (triangles), for the Sgr field of MUSKKK with $0.70 \leq V - I \leq 0.95$ (open circles), and for the control field of MUSKKK (filled circles). They have been scaled to the MUSKKK Sgr field over $15 < V < 18$ mag.

that is much smaller than the other three LFs, it appears less significant.

A second test of the nature of the RHB comes from the radial distribution of its members, with respect to the radial distributions of the other principal sequences of M54 and Sgr. Figure 11 illustrates the cumulative radial distributions of the M54 RGB (thin solid line), M54 BHB (short dashed line), Sgr RGB (dotted line), Sgr red clump (long dashed line), and the anonymous RHB (thick solid line). A K–S test indicates that the radial distribution of the RHB is different from those of the M54 RGB and BHB at the >99.9% confidence level. However, the distribution of the RHB stars is

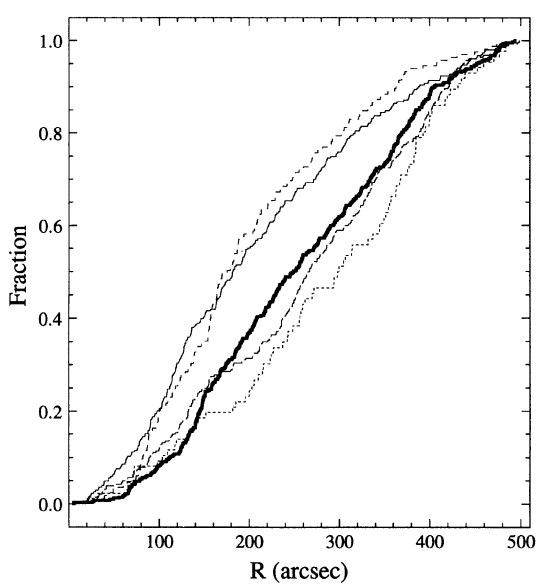

FIG. 11. The cumulative radial distributions of the M54 RGB (thin solid line), M54 BHB (short dashed line), Sgr RGB (dotted line), Sgr red clump (long dashed line), and the anonymous RHB (thick solid line). The RHB star distribution follows those of the Sgr stars, suggesting that the RHB is associated with Sgr and not M54.

not significantly different from those of the Sgr RGB and the Sgr red clump. We take this as further evidence that the RHB belongs to Sgr.

A final test involves a comparison between the HB of M68 (Walker 1994) and that of M54. The globular cluster M68 has [Fe/H]$=-2.1$ and an HB morphology like that of the M54 BHB plus the anonymous RHB. Shifting the M68 HB by $\Delta V=2.50$ and $\Delta(V-I)=0.09$ yields the best match with the BHB of M54, as shown in Fig. 6(a). The dashed box on the HB represents the location of the M68 RR Lyrae variables, as given by Walker (1994). For 40 such stars, he finds $\langle V(\mathrm{RR})\rangle = 15.64 \pm 0.01$. If we apply $\Delta V=2.50$ to this, we infer an RR Lyrae magnitude of $V=18.14$ for M54, which is in good agreement with our value of $V(\mathrm{RR})=18.17$, derived assuming that all 16 RR Lyraes measured in Fig. 3 belong to M54. Clearly, the anonymous RHB lies well below the M68 fiducial (≈ 0.15 mag), suggesting that the RHB is not associated with M54. This behavior is supported by applying the same comparison with the HBs of NGC 5053 (Sarajedini & Milone 1995) and NGC 5897 (Ferraro *et al.* 1992). The offsets applied to these sequences imply $V(\mathrm{RR}) = 18.20$ and $V(\mathrm{RR})=18.10$, respectively, for M54, again supporting our derived M54 $V(\mathrm{RR})$ value.

The evidence presented thus far suggests that the RHB is, in fact, associated with the Sgr dwarf galaxy, not M54, implying that M54 has few, if any, red HB stars. This will, of course, affect the apparent HB morphology of M54, as measured by the index of Lee *et al.* (1994, and references therein), $(B-R)/(B+V+R)$. First, we note that the known M54 RR Lyraes are all located outside 50 arcsec of the cluster center. Restricting ourselves to this region on our Tek1024 frames, we find 105 BHB stars and 16 RR Lyrae variables. Assuming that $R=0$, we find $(B-R)/(B+V+R) = 0.87$. There is some uncertainty in this value for the following reasons. First, there are likely to be *bona fide* RR Lyrae variables that Sawyer-Hogg (1973) did not identify as such; in addition, some of the RR Lyraes may in reality belong to Sgr. Last, we cannot be sure that $R=0$ exactly. However, $(B-R)/(B+V+R)$ is certainly larger than 0.22, as quoted by Preston *et al.* (1991) on the assumption that the RHB belongs to M54. Regardless, our adopted $V(\mathrm{RR})$ of M54 is still valid, because it is supported by the results of the BHB comparisons with M68, NGC 5053, and NGC 5897. We note, in passing, that M54 joins NGC 4147 as the two most metal-poor Oosterhoff type I clusters among the Galactic globulars (Castellani & Quarta 1987).

Returning to a discussion of Sgr, we conjecture that the RHB represents some older or more metal-poor population, as compared with the Sgr red clump stars. If the latter is true, then there should also be a third RGB present in Fig. 3, lying blueward and brightward of the dominant Sgr RGB. Such a sequence is evident in Figs. 3 and 7. Between the RGBs of M54 and Sgr, there appears to be an additional scattering of RGB stars, which is also weakly present in the Sgr CMD of MUSKKK. Based upon its location in Fig. 8, this second Sgr RGB seems to have a spread of metallicities, with a mean of [Fe/H]≈ -1.3. The K–S test indicates that the radial distributions of the Sgr red clump, RGB, RHB, and the [Fe/H] ≈ -1.3 red giant stars are not significantly different. As a

TABLE 3. Distances to M54 and Sgr in Kpc.

$M_V(RR)$	M54	Sgr RHB	Sgr Clump
+0.6	27.0 ± 1.0	28.5 ± 1.1	29.3 ± 0.9
0.15[*Fe/H*]+ 1.01	25.3 ± 0.9	25.8 ± 1.0	25.1 ± 0.8
0.17[*Fe/H*]+ 0.82	28.0 ± 1.0	28.5 ± 1.1	27.6 ± 0.9
0.30[*Fe/H*]+ 0.94	29.5 ± 1.1	29.2 ± 1.1	26.9 ± 0.8

result, the latter stars may be associated with the RHB of Sgr.

In order to investigate this possibility further, we compare the relative numbers of stars on the various CMD sequences attributed to Sgr. We count the numbers of stars in the dashed areas of Fig. 7, which indicate the Sgr metal-rich (MR) RGB and the intermediate metallicity (IM) RGB. These regions contain 83 and 90 stars, respectively. In contrast, the control field of MUSKKK contains 11 and 9 stars, respectively, in these regions.[4] The overabundance of stars in the Sgr fields suggests that these are real intermediate-metallicity members of Sgr. Calculating the numbers of stars on the RHB and the Sgr red clump is more problematic. The former is predominantly affected by the foreground field population, while the latter is influenced by the Sgr MR RGB, the IM RGB, and the RGB of M54. To deconvolve all of these populations, we first select all stars in Fig. 7 with $18.1<V<18.4$. A color histogram of these stars is constructed, and the peaks that correspond to the features of interest are isolated. Gaussian distributions are fitted to the points in the histogram around each peak. The area under these distributions is then the total number of stars associated with each feature. Thus, we can form the following ratios: $N^{\rm MR}_{\rm RGB}/N_{\rm clump}=0.43\pm0.06$ and $N^{\rm IM}_{\rm RGB}/N_{\rm RHB}=0.58\pm0.08$, which corresponds to a marginally significant difference of 0.15 ± 0.10. If we include stars on the redward extension of the MR RGB with $V-I>2.2$, we find $N^{\rm MR}_{\rm RGB}/N_{\rm clump}=0.52\pm0.06$, leading to a difference of only 0.06 ± 0.10. The similarity of these ratios indicates that it is plausible to consider the intermediate abundance RGB to be associated with the RHB.

Turning now to the age of Sgr, the work of MUSKKK suggests that the dominant population in Sgr has an age of ≈10 Gyr, which is consistent with a red clump HB morphology at [Fe/H]≈−0.5 and a red HB at [Fe/H]≈−1.3. The latter situation may resemble Galactic globular clusters with red HBs, [Fe/H]≈−1.3, and ages somewhat younger than the mean, such as NGC 362, Eridanus, and Pal 4 (see Sarajedini *et al.*). However, more precise turn-off photometry is required to answer this question definitively. We note that this arrangement is the opposite of that in the Carina dSph (Smecker-Hane *et al.* 1994), where two populations of similar abundance, but different age, produce distinct HB populations and a single RGB.

The HB magnitudes derived in Sec. 4 for M54, the Sgr clump, and the RHB (now associated with Sgr) are nearly equal, suggesting that M54 and Sgr are at about the same distance from the Sun. A more accurate assessment depends on the M_V(RR)−[Fe/H] relationship one chooses to adopt. Table 3 shows the derived distances, in Kpc, of the three populations, assuming $E(B-V)=0.13$, $A_V=3.2E(B-V)$, [Fe/H]=−1.79 (M54), −0.52 (Sgr clump), and −1.3 (Sgr RHB). In addition, we have used four different values for the luminosity of the RR Lyrae variables: (1) M_V(RR)=+0.6, (2) M_V(RR)=0.15[Fe/H]+1.01 (Carney *et al.* 1992), (3) M_V(RR)=0.17[Fe/H]+0.82 (Lee *et al.* 1990), and (4) M_V(RR)=0.30[Fe/H]+0.94 (Sandage 1993). Our data has yielded a value of $\langle V(\rm RR)\rangle=18.17\pm0.05$ for M54, but, in the case of the Sgr RHB and red clump, we must estimate the magnitude of the equivalent RR Lyrae stars. To do this, we employ the synthetic red HB models of Lee (1994, private communication), to adjust the Sgr RHB fainter by 0.04 mag and the red clump fainter by 0.11 mag. The resultant inferred values are $\langle V(\rm RR)\rangle=18.29\pm0.05$ for the RHB population and $\langle V(\rm RR)\rangle=18.35\pm0.02$ for the red clump, where the errors do not reflect the uncertainties in the estimated offsets. The errors in the distances given in Table 3 reflect the quoted uncertainties in the input parameters.

Considering the similar distance estimates for M54 and Sgr in Table 3, the similarities in radial velocity, 131±4 km s^{-1} (Webbink 1981) and 140±2 km s^{-1} (IGI), respectively, and the fact that M54 lies at the center of the densest lump in the IGI isopleths, it seems quite likely that M54 is itself a part of the Sgr dwarf galaxy. Perhaps it represents the oldest, most metal-poor, epoch of star formation in Sgr, essentially the nucleus about which the rest of the galaxy condensed. This raises the question of whether Sgr is a nucleated dwarf galaxy. Freeman (1993) suggested that the nuclei of such galaxies may closely resemble globular clusters, and, in fact, "produce" them when nucleated dwarf galaxies are accreted by larger galaxies. However, the colors of these nuclei are usually very similar to that of the surrounding dwarf field stars, whereas M54 appears considerably bluer than the surrounding Sgr field. Thus, M54 is likely to be a more luminous version of Fornax-like globulars, rather than a galactic nucleus.

If we correct Djorgovski's (1993) M_V estimate of M54, which employed $V_{\rm HB}=17.71$, we find $-9.75>M_V>-10.09$, depending on which of the above-mentioned M_V(RR)−[Fe/H] relations is used. Regardless, the range of possible integrated luminosities for M54 includes the luminosity of ω Centauri, (see Djorgovski 1993), which is known to have a metallicity spread among its stars. Thus, the fact that M54 also appears to have a metallicity spread has important implications for studies that seek to pinpoint a minimum mass above which globular clusters enrich themselves in heavy elements. Furthermore, M54 is two magnitudes more luminous than the brightest globular cluster in Fornax (Buonanno *et al.* 1985).

Meanwhile, if the entire stellar population of Sgr is as metal rich as [Fe/H]≈−0.5, then the M_V−[Fe/H] relation of Zinn (1993, and references therein) predicts an absolute luminosity of $M_V\approx-20$ mag. Even the lower abundance estimates of IGI and MUSKKK predict $M_V\approx-16$ mag. Yet, based on counting HB stars on their UK Schmidt plates, IGI found a luminosity of $M_V\approx-13$ mag. Perhaps, earlier in its history, Sgr was much more luminous than it appears today. Subsequent interactions with the galaxy could have stripped away a significant portion of its original mass. Clearly, its high abundance for its luminosity, and its bright globular

[4]See footnote 3.

cluster member, M54, indicate that Sagittarius is unusual, relative to other dwarf spheroidal satellite galaxies of the Milky Way, and is therefore worthy of further study.

We are grateful to Taft Armandroff, Nick Suntzeff, Gary Da Costa, Ed Olszewski, and Mario Mateo (the referee) for useful suggestions, which greatly improved this work. We also acknowledge Bill Harris for providing valuable details of his previous work on M54. We are indebted to the director of CTIO for granting us two "Director's Discretionary" nights on the CTIO 0.9 m telescope for this project.

REFERENCES

Bica, E., Ortolani, S., & Barbuy, B. 1994, A&AS, 106, 161
Buonanno, R., Corsi, C. E., Fusi Pecci, F., Hardy, E., & Zinn, R. J. 1985, AAp, 152, 65
Burstein, D., & Heiles, C. 1982, AJ, 87, 1165
Carney, B. W., Storm, J., & Jones, R. V. 1992, ApJ, 386, 663
Castellani, V., & Quarta, M. L. 1987, A&AS, 71, 1
Cudworth, K. M., & Rees, R. 1990, AJ, 99 1491
Da Costa, G. S., & Armandroff, T. E. 1990, AJ, 100, 162
Dean, J. F., Warren, P. R., & Cousins, A. W. J. 1978, MNRAS, 183, 569
Djorgovski, S. G. 1993, in Structure and Dynamics of Globular Clusters, ASP Conf. Ser., edited by S. G. Djorgovski and G. Meylan (ASP, San Francisco), Vol. 50, p. 373
Ferraro, F. R., Fusi Pecci, F., & Buonanno, R. 1992, MNRAS, 256, 376
Freeman, K. C. 1993, in The Globular Cluster–Galaxy Connection, ASP Conf. Ser., edited by G. H. Smith and J. P. Brodie (ASP, San Francisco), Vol. 48, p. 608
Harris, W. E. 1975, ApJS, 29, 397
Ibata, R. A., Gilmore, G., & Irwin, M. J. 1994, Nature, 370, 194 (IGI)
Keeping, E. S. 1962, Introduction to Statistical Inference (Van Nostrand, Princeton), p. 202
Landolt, A. U. 1992, AJ, 104, 340
Lee, Y.-W. 1990, ApJ, 363, 159
Lee, Y.-W. 1994, private communication
Lee, Y.-W., Demarque, P., & Zinn, R. J. 1990, ApJ, 350, 155
Lee, Y.-W., Demarque, P., & Zinn, R. J. 1994, ApJ, 423, 248
Mateo, M., Udalski, A., Szymanski, M., Kaluzny, J., Kubiak, M., & Krzeminski, W. 1995, AJ (MUSKKK) (in press)
Preston, G. W., Shectman, S. A., & Beers, T. C. 1991, ApJ, 375, 121
Sandage, A. 1993, AJ, 106, 703
Sarajedini, A. 1994, AJ, 107, 618
Sarajedini, A., & Da Costa, G. S. 1991, AJ, 102, 628
Sarajedini, A., Lee, Y.-W., & Lee, D.-H. 1994, in preparation
Sarajedini, A. & Milone, A. A. E. 1995, AJ, 109, 269
Sarajedini, A. & Norris, J. E. 1994, ApJS, 93, 161 (SN94)
Sawyer-Hogg, H. 1973, A Third Catalogue of Variable Stars in Globular Clusters Comprising 2119 Entries, Publications of the David Dunlap Observatory, Vol. 3, No. 6 (University of Toronto, Toronto)
Smecker-Hane, T. A., Stetson, P. B., Hesser, J. E., & Lehnert, M. D. 1994, AJ, 108, 507
Stetson, P. B. 1987, PASP, 99, 191
Stetson, P. B. 1990, PASP, 102, 932
Walker, A. R. 1994, AJ, 108, 555
Webbink, R. F. 1981, ApJS, 45, 259
Zinn, R. J. 1993, in The Globular Cluster–Galaxy Connection, ASP Conf. Ser., edited by G. H. Smith and J. P. Brodie (ASP, San Francisco), Vol. 48, p. 302
Zinn, R. J., & West, M. J. 1984, ApJS, 55, 45

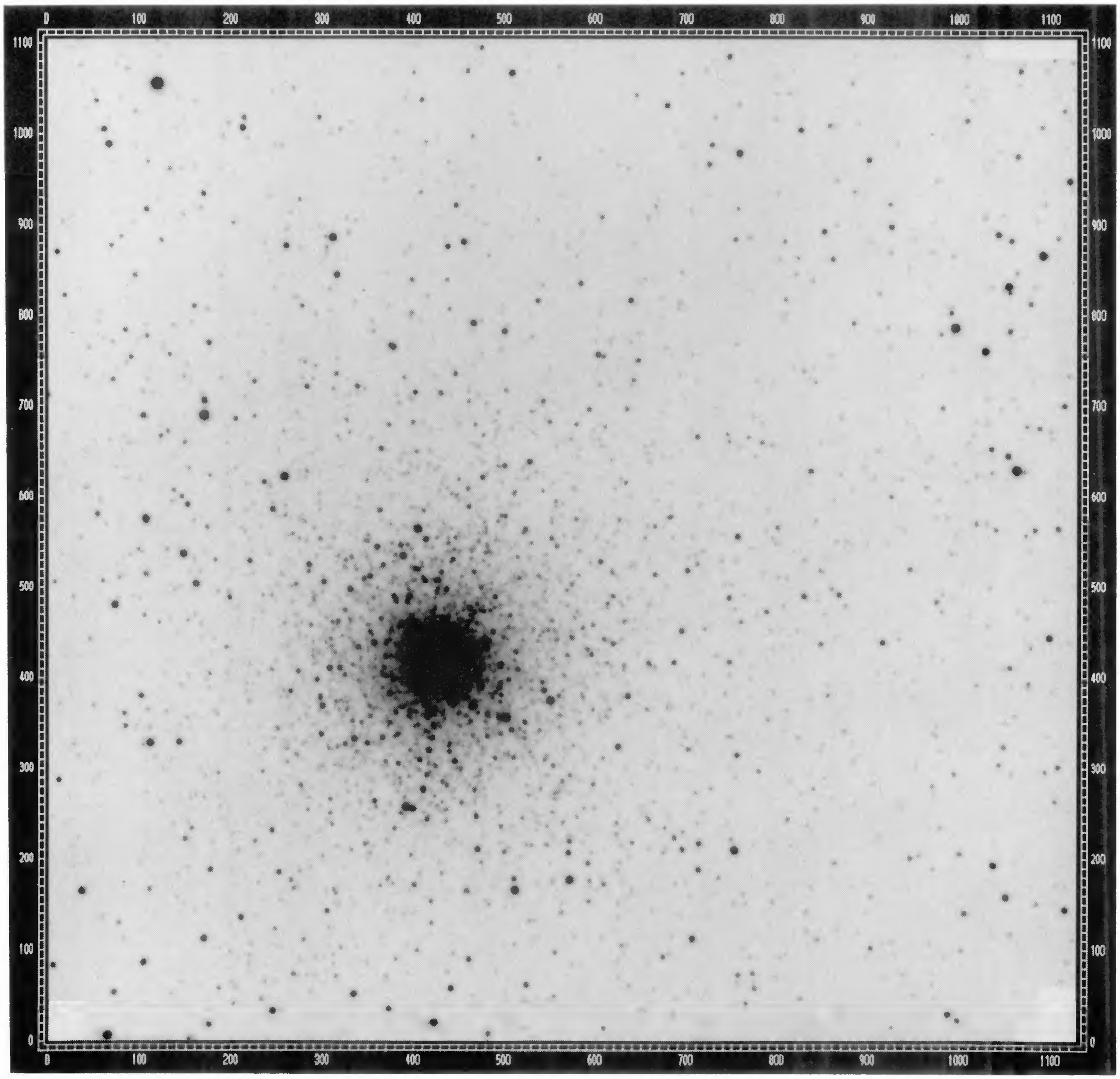

FIG. 1. *V* band reproduction of the observed M54 field. North is to the left and east is at the bottom. The field is ~6.8 arcmin square.

A. Sarajedini and A. C. Layden (see page 1086)

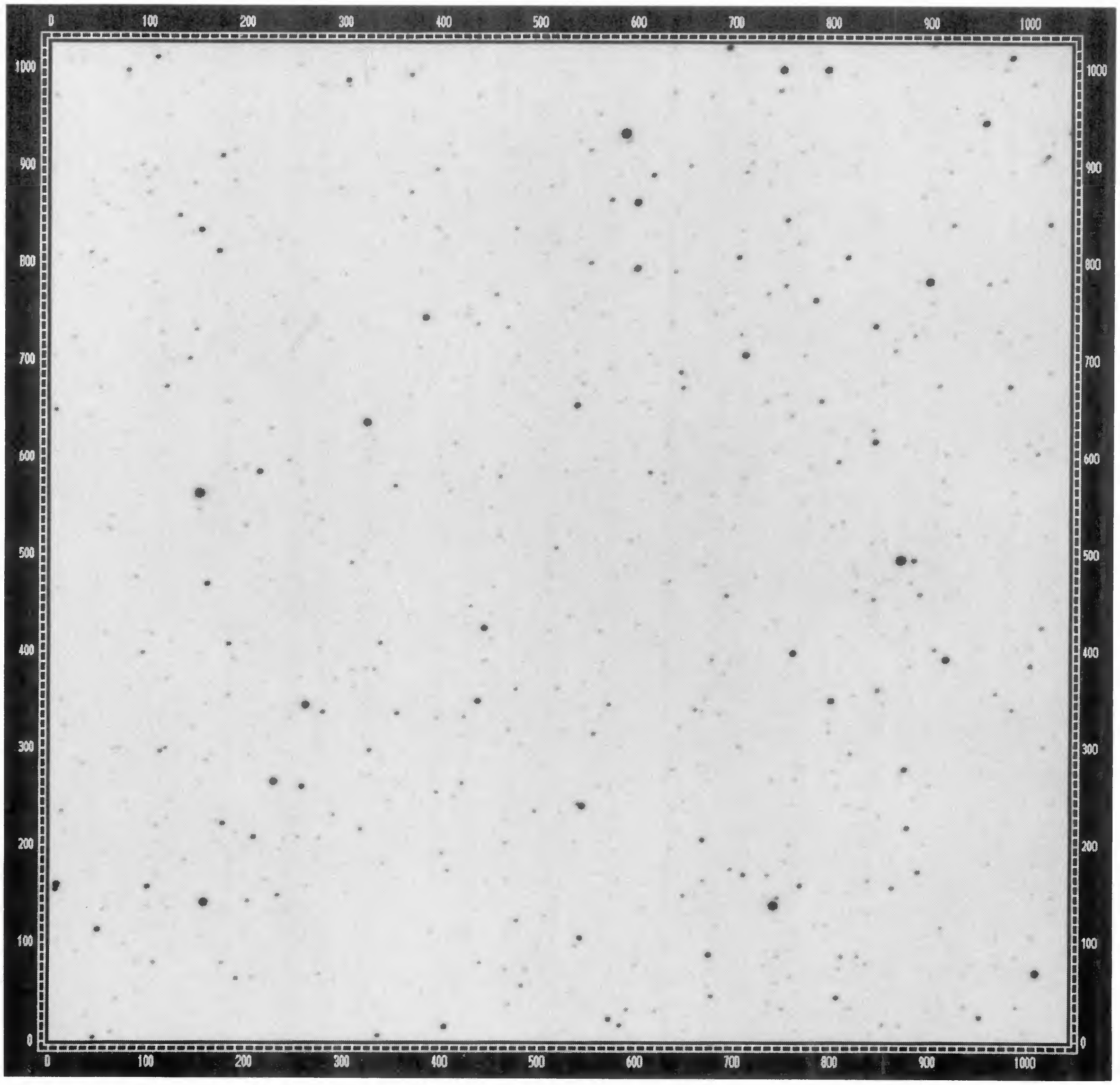

FIG. 2. *V* band reproduction of the off-cluster field located 12 arcmin north of M54. North is to the left and east is at the bottom.

A. Sarajedini and A. C. Layden (see page 1086)

THE ASTRONOMICAL JOURNAL

FOUNDED BY B. A. GOULD
1849

:UME 109 **March 1995~No. 1671** *NUMBER 3*

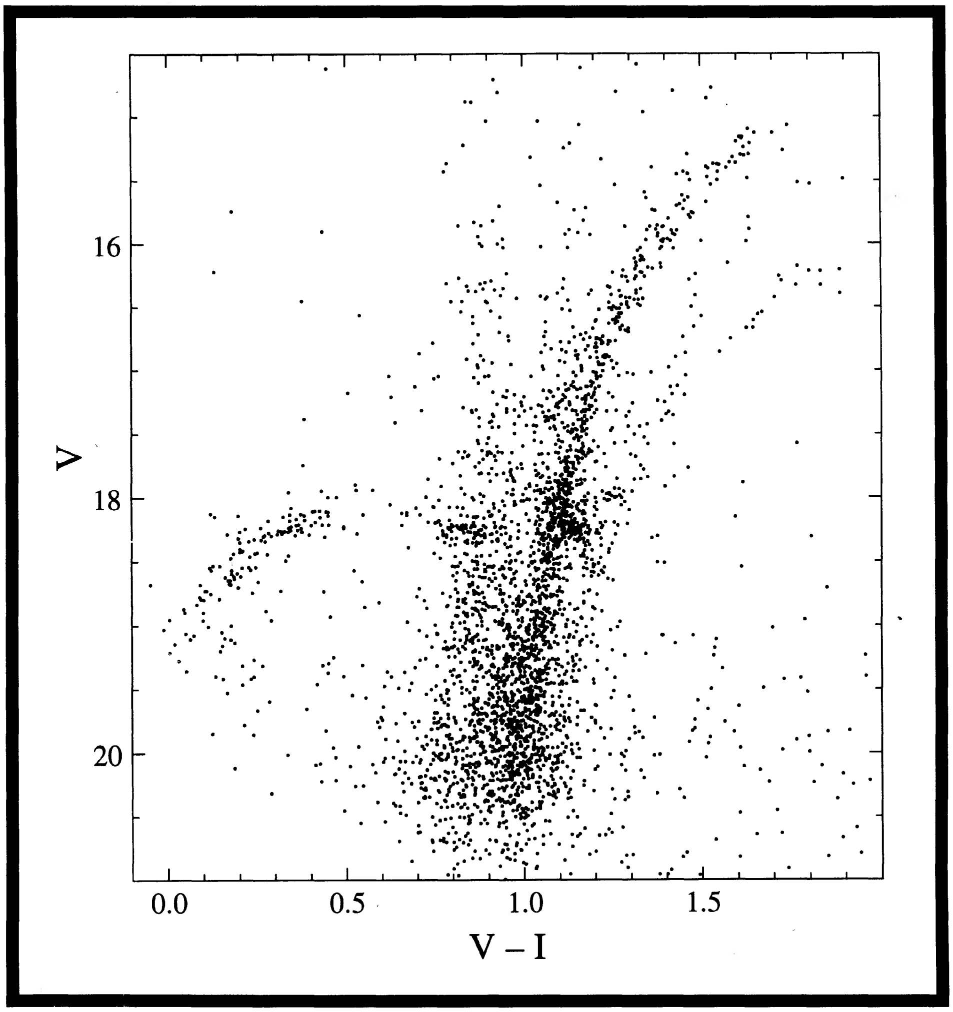

(See Page 1086)

Published for the
AMERICAN ASTRONOMICAL SOCIETY
by the
AMERICAN INSTITUTE OF PHYSICS